Direct Observation of Surface Chemical Order by Scanning Tunneling Microscopy

M. Schmid, H. Stadler, and P. Varga
Institut für Allgemeine Physik, Technische Universität Wien, A-1040 Wien, Austria
(Received 4 August 1992)

We present the first scanning tunneling microscopy (STM) study which allows clear discrimination of two chemical species in a metal alloy. Special tunneling conditions, which we attribute to an adsorbate at the STM tip, cause a difference in corrugation between Pt and Ni atoms of 0.3 Å. The STM data reveal chemical short-range order at the surface, which is in agreement with embedded atom simulations and can be understood as small domains of an $L1_0$ ordered phase.

PACS numbers: 61.16.Ch, 61.66.Dk, 68.35.−p

Scanning tunneling microscopy is a powerful technique for the study of solid surfaces. While STM readily delivers geometrical data on both metals and semiconductors, information about the chemical structure was previously restricted to a few semiconducting systems, where tunneling spectroscopy [1] and laser excitation [2] allow discrimination between different species. These methods are not successful on metal surfaces, since (a) metal wave functions are too delocalized and (b) atomic resolution on metals usually limits the tunneling voltage to below 100 mV.

Discrimination of atomic species from their different corrugation has not been successful previously. Parkinson reports a larger variation of corrugations on WSeS compared to WS_2 and WSe_2, but it was impossible to discriminate between the two species [3]. Also previous STM studies of Pt-Ni alloys [4] show little variation between the corrugation of individual atoms. On a $c(2\times2)$ AuCu layer on Cu(100), a weakly discernible difference between the corrugations of Cu and Au has been reported, but this may be also caused by different core positions [5].

Triggered by theoretical predictions of differences between bulk and surface order, the study of surface chemical order has been very active in recent years. Most previous studies of surface chemical order on metals were based on diffraction techniques, such as (spin-polarized) low-energy electron diffraction [6,7] and glancing incidence x-ray scattering [8,9]. Since these k-space methods average over large regions of the sample, interpretation of their results is limited to statistical criteria.

The only real-space technique resolving individual metal atoms with information on their chemical nature was the field ion microscope (FIM). Since different species appear with different brightnesses in FIM images, the FIM can be used for the study of chemical ordering in real space [10]. The FIM is limited to very sharp tips, and it is impossible to map a flat facet larger than a few nanometers. This is a problem in the study of surface order, where large flat surfaces are both desirable (from a theoretical point of view) and sometimes unavoidable due to faceting while annealing the sample. Similar problems also arise with the position-sensitive atom probe (POSAP) [11], a combination of FIM and mass spectroscopy.

In this Letter we show for the first time a clear discrimination between different chemical species in a metal alloy by scanning tunneling microscopy. We show that different corrugations of Pt and Ni atoms on an alloy single crystal occur in atomically resolved images under certain tip conditions, which enables us to study the surface order of this sample.

Our results were achieved using a customized prototype of a commercial scanning tunneling microscope (Omicron micro-STM) operated in constant current mode with positive tip bias. The tip was electrochemically etched from tungsten wire and cleaned in vacuum by field evaporation (300 V) and voltage pulses (3 to 10 V) while tunneling. Sample preparation and STM analysis were done in ultrahigh vacuum at a base pressure below 1×10^{-10} mbar. The sample, a $Pt_{25}Ni_{75}(111)$ single crystal, was prepared by repeated cycles of sputtering (500 eV Ar^+) and annealing (last annealing temperature 780 K for 5 min). Low-energy electron diffraction (LEED) does not show any superstructure spots, which might indicate chemical ordering.

After extensive surface preparation, atomically resolved STM images on this surface [Fig. 1(a)] are routinely achieved at rather low tunneling resistance (50 to 300 kΩ). These images show atomic corrugation of 0.1 to 0.2 Å, with very little variation between individual atoms. Tip conditions leading to such images are usually rather stable; subsequent images of the same surface region are virtually identical. At higher tunneling resistance, the atomic corrugation gradually disappears.

If the surface is prepared less thoroughly, but still sufficiently to achieve "clean" Auger spectra, tunneling conditions are less stable. We often observe sudden changes in image quality, especially when the tip reaches a step. We attribute this to adsorbates hopping between sample and tip or between tip sites. Adsorbates often show a preference for step edges (we have also observed this for sulfur on the same sample [12]), which easily explains why tip conditions are most unstable near steps.

Nevertheless, at a tunneling resistance below approximately 100 kΩ, atomic resolution similar to Fig. 1(a) can also be achieved on this surface although it is not as clean

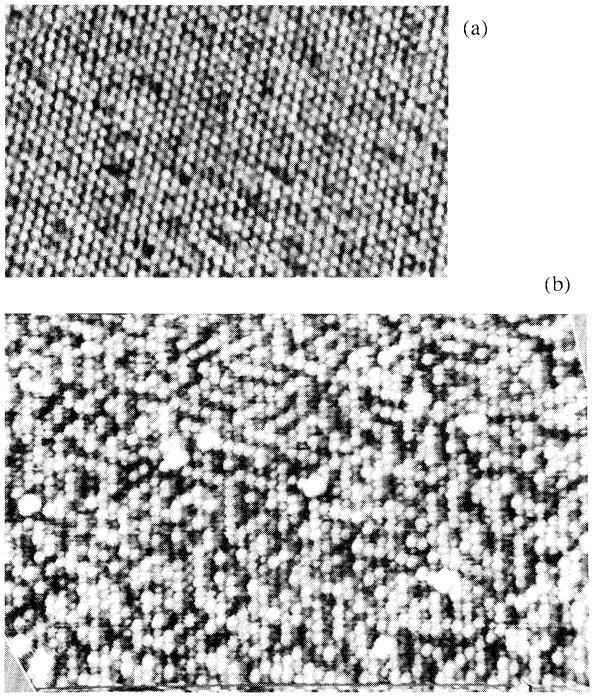

FIG. 1. STM constant current topographs of the (111) surface of a $Pt_{25}Ni_{75}$ single crystal. Tunneling voltage/current and sample treatment: (a) 0.5 mV/7 nA, thoroughly cleaned; (b) 5 mV/16 nA, less cleaning. Image sizes are 100 Å×70 Å and 125 Å×100 Å. Both images have been slightly high-pass filtered; image (b) has been distorted to correct for drift and creep of the STM.

as in Fig. 1(a). These images are slightly more noisy than Fig. 1(a), but the variation between the corrugation of individual atoms is still small. With somewhat higher tunneling resistance (typically 300 kΩ), the situation changes drastically: If the tip is still stable enough for atomically resolved images, we can find large variations of the corrugation between different atoms. As Fig. 1(b) shows, two distinct species, "bright" (high corrugation) and "dark" (low corrugation) atoms, can be distinguished; furthermore, a few white blobs (probably impurities) can be observed. The bright and dark species show some short-range order; i.e., there are alternating chains (up to seven atoms long) of the two species in many parts of the image.

For quantification, we have used image processing techniques to determine the maximum corrugation (z coordinate of the "top" of the atom) within each lattice cell. The result of this procedure is a histogram of corrugation values. The histograms for the STM images in Figs. 1(a) and 1(b) are shown in Figs. 2(a) and 2(b), respectively. The two peaks in Fig. 2(b) clearly vindicate two species with different corrugation. Thus it is likely that these different species correspond to the different elements Pt and Ni. This assumption is confirmed by a

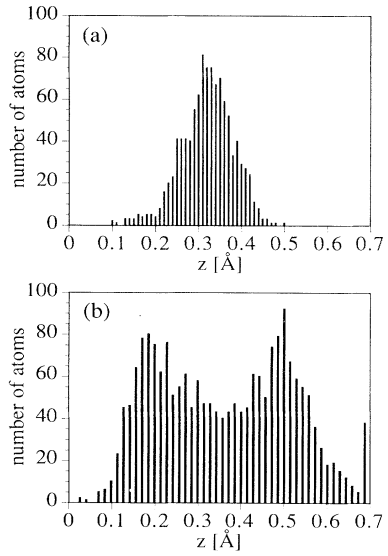

FIG. 2. Histograms of the highest tip position z (maximum corrugation) within each lattice cell in Figs. 1(a) and 1(b), respectively. The offset of the z scale is arbitrary. The two maxima in histogram (b) correspond to the "dark" (left peak) and "bright" (right peak) species of Fig. 1(b); all corrugations above 0.7 Å ("white blobs") have been included in the rightmost column.

comparison between the STM image and simulations of chemical ordering on this sample (see Fig. 3 and below).

Fitting two Gaussians into the histogram yields 47.2 dark and 50.9 bright lattice sites; 1.9% of the lattice sites are covered by the white blobs (in the right edge of the histogram). This result is close to a manual evaluation (counting dark and bright atoms). Based on counting statistics and results of different image processing tech-

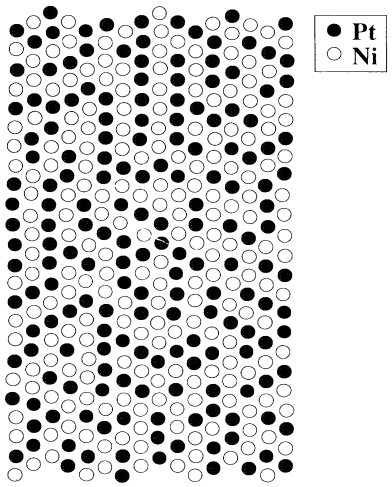

FIG. 3. Atomic arrangement on the (111) surface calculated by Monte Carlo simulations with embedded atom potentials. Bulk composition is assumed as 37% Pt and 63% Ni; temperature is 420 K.

niques we have estimated the error of this analysis, which yields more than 80% probability for the bright species being more abundant than the dark one; a "reversed" situation with 47% bright and 51% dark is very improbable.

Conventional surface analysis on this sample reveals platinum enrichment to some 50% Pt in the first monolayer, which is caused by both preferential sputtering and segregation of Pt [13,14]. This supports the correlation of Pt and Ni with the two distinct species, but it does not help to decide which element belongs to which species. However, comparing images taken after different treatment of the sample, we could find that the fraction of dark sites increases with sputter time. Since preferential sputtering causes gradual Pt enrichment of the first layers, we will tentatively identify the dark species as Pt and the bright species as Ni. This assumption is confirmed by the fact that the simulation calculations show the best fit to Fig. 1(b) if the surface concentration of Pt is definitely below 50% [47% in Fig. 3, which perfectly matches the fraction of dark sites in Fig. 1(b)].

Since our simulation calculations (described below) show that the vertical position of the Pt and Ni cores is virtually identical, the different corrugations of the two species in Fig. 1(b) cannot be attributed to their geometrical position. The difference of atomic radii is only half the observed corrugation difference (0.14 Å) and would result in bright Pt atoms. It is also unlikely that the contrast mechanism is due to their different electronic structure, since both are *d* metals with similar density of states near the Fermi level. Deformation of the crystal lattice is expected to be strongest at low tunneling resistance (short gap distance); therefore, it cannot be used to explain a contrast mechanism which occurs at higher tunneling resistance than usual. A barrier height effect seems implausible at the low tunneling resistance, since tip-sample distance is very short. Furthermore, all these effects cannot explain why we could never obtain chemically resolved images in many weeks of STM work on the thoroughly cleaned surface.

Experimental evidence rather points to the effect of an adsorbate on the tip for the explanation of chemically resolved images like Fig. 1(b): (1) Such images have not been obtained after thorough cleaning of the surface; (2) tip conditions leading to such images are rather short lived; and (3) adsorbates are only stable at a tunneling resistance above a certain limit [15], which explains the dependence on tunneling resistance. Nevertheless, even at a tunneling voltage of 300 kΩ the tip-sample distance is low enough for some interaction between adsorbate and tip (calculations for an Al tip on Al yield approximately 6 Å between atom core positions [16]).

Assuming an adsorbate at the tip, which is close to the surface, one may expect that the adsorbate tends to form a chemical bond more likely with one element than with the other (as long as the adsorbate stays on the tip, we should speak of a "precursor," similar to a hydrogen bridge, rather than of a chemical bond). This "chemical bond" will increase the density of states between the adsorbate and the surface, and possibly move the adsorbate closer to the surface. Both mechanisms lead to a higher tunneling current, which is imaged as higher corrugation in a constant current topograph. In our case of Pt and Ni, most adsorbates will rather form a chemical bond with Ni than with the noble Pt, leading to the tentative conclusion that the bright species is Ni. This agrees with our conclusions drawn above.

We may only speculate about the nature of the adsorbate leading to the chemically resolved images. The adsorbate must be sufficiently immobile at the tip to remain at a single position for the many seconds required to record an STM image. Likely candidates are sulfur (which segregates to the sample surface at high temperature) and oxygen. These electronegative adsorbates have also been suspected in a case of unusual effects in scanning tunneling spectroscopy [17].

For comparison with STM data, we have performed simulations of chemical order in Pt-Ni. A Monte Carlo code using embedded atom potentials [18] has been employed to simulate the chemical order of a (111)-oriented crystal slab. The program is based on comparison between chemical potential and substitutional energy, accounting for relaxation [19]. For the calculations presented in Fig. 3 we have assumed a temperature of 420 K and a bulk composition of $Pt_{37}Ni_{63}$ (this is different from the true bulk composition but rather represents the surface layers, which are Pt enriched by preferential sputtering [4,13]).

The simulations verify segregation of Pt to the surface and Ni enrichment of the second layer, which has been found for $Pt_xNi_{1-x}(111)$ surfaces by experimental [20,21] and theoretical [22,23] methods. The simulation (Fig. 3) also shows surface ordering of the kind observed by STM, which makes us sure that the observed contrast is indeed due to the two chemical species.

The reason for this kind of order may be explained from the phase diagram of Pt-Ni [24], which is similar to the Cu-Au system, a prototype for chemical order and phase transitions: Below 930 K, $Pt_{50}Ni_{50}$ forms an ordered $L1_0$ phase, which consists of alternating Pt and Ni layers in the [001] direction (Fig. 4). The (111) face of such a crystal consists of alternating rows of Pt and Ni in the $[\bar{1}10]$ direction (1×2 superstructure; Fig. 4), which indicates why these rows occur on the surface investigated. The simulations also show such rows in deeper layers, (continuation of the $L1_0$ structure), but the bulk of the sample (25% Pt) cannot exhibit this structure. Since the $L1_0$ ordering is due to Pt enrichment at the surface, we may speak of a kind of surface-induced order.

The $L1_0$ phase is tetragonal, however, whereas the bulk of our crystal has cubic symmetry (fcc, independent of any possible $L1_2$ bulk order). This means that the (111) face of the $L1_0$ phase is somewhat distorted, compared to the threefold symmetry of the substrate (Fig. 4). This geometrical constraint limits the size of $L1_0$ domains,

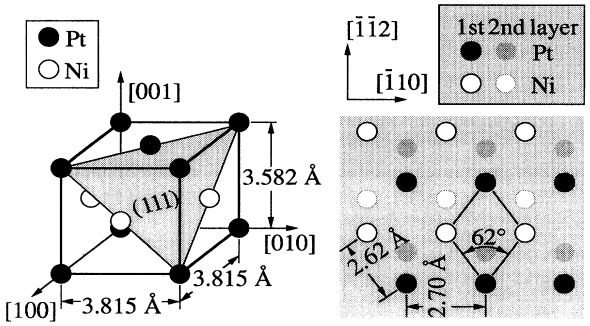

FIG. 4. Schematic view of the $L1_0$ structure of $Pt_{50}Ni_{50}$ (left-hand side) and the corresponding (111) surface obtained by a cut through this structure (right-hand side). Lattice constants are from Ref. [25].

since the misfit between the distorted surface layers and the bulk induces lateral strain. We believe that this is the main reason for the short correlation length, which occurs although the surface concentrations are well inside the ordered region of the phase diagram at annealing temperature and below.

Since there are only small domains of (1×2) superstructure, the Fourier transform of Fig. 1(b) shows very weak and diffuse superstructure spots at $(0,\frac{1}{2})$ and equivalent positions. This fact, which is equivalent to the short correlation length, explains why we could not observe the order by LEED.

To summarize, we have presented the first example of chemically resolved scanning tunneling microscopy on a metal alloy. On the (111) surface of a $Pt_{25}Ni_{75}$ single crystal, we have found a difference of corrugation between Pt and Ni atoms of 0.3 Å, occurring at higher tunneling resistance than normally used for atomically resolved topographs of the same surface. This is attributed to the interaction of an adsorbate at the tunneling tip with the individual surface atoms. The discrimination between two different atomic species has enabled us to study the surface chemical order, revealing short-range ordering on this surface.

The authors would like to thank Stephen M. Foiles (Sandia National Laboratories, Livermore) for supplying us with the computer code and for his substantial help in implementing the embedded atom method, and G. S. Sohal for the crystal. This work was supported by the "Fonds zur Förderung der Wissenschaftlichen Forschung" (Austrian Science Foundation) under Project No. P8147.

[1] R. M. Tromp, J. Phys. Condens. Matter **1**, 10211 (1989).
[2] L. L. Kazmerski, J. Vac. Sci. Technol. B **9**, 1549 (1991).
[3] B. A. Parkinson, J. Am. Chem. Soc. **112**, 1030 (1990).
[4] M. Schmid, A. Biedermann, H. Stadler, and P. Varga, Phys. Rev. Lett. **69**, 925 (1992); M. Schmid, A. Biedermann, H. Stadler, C. Slama, and P. Varga, Appl. Phys. A **55**, 468 (1992).
[5] D. D. Chambliss and S. Chiang, Surf. Sci. Lett. **264**, L187 (1992).
[6] V. S. Sundaram, B. Farell, R. S. Alben, and D. W. Robertson, Phys. Rev. Lett. **31**, 1136 (1973).
[7] S. F. Alvorado, M. Campagna, A. Fattah, and W. Uelhoff, Z. Phys. B. **66**, 103 (1987).
[8] R. Feidenhans'l, Surf. Sci. Rep. **10**, 105 (1989).
[9] X-M. Zhu, H. Zabel, I. K. Robinson, E. Vlieg, J. A. Dura, and C. P. Flynn, Phys. Rev. Lett. **65**, 2692 (1990).
[10] T. T. Tsong and E. W. Müller, Appl. Phys. Lett. **9**, 7 (1966); J. Appl. Phys. **38**, 545 (1967); **38**, 3531 (1967).
[11] A. Cerezo, J. M. Hyde, M. K. Miller, G. Beverini, R. P. Setna, P. J. Warren, and G. D. W. Smith, Surf. Sci. **226**, 481 (1992).
[12] M. Schmid, A. Biedermann, and P. Varga (to be published).
[13] P. Weigand, P. Novacek, G. van Husen, T. Neidhart, L. Z. Mezey, W. Hofer, and P. Varga, Nucl. Instrum. Methods Phys. Res., Sect. B **64**, 93 (1992).
[14] P. Weigand, C. Nagl, M. Schmid, and P. Varga, Fresenius J. Anal. Chem. (to be published).
[15] J. A. Stroscio and D. M. Eigler, Science **254**, 1319 (1991).
[16] E. Tekman and S. Ciraci, Phys. Rev. B **42**, 1860 (1990).
[17] R. M. Tromp, E. J. van Loenen, J. E. Demuth, and N. D. Lang, Phys. Rev. B **37**, 9042 (1988).
[18] S. M. Foiles, M. I. Baskes, and M. S. Daw, Phys. Rev. B **33**, 7983 (1986); **37**, 10378(E) (1988).
[19] S. M. Foiles, in *Surface Segregation Phenomena,* edited by P. A. Dowben and A. Miller (CRC, Boca Raton, FL, 1990), p. 79.
[20] Y. Gauthier *et al.*, Surf. Sci. **162**, 342 (1985); Y. Gauthier, Y. Joly, R. Baudoing, and J. Rundgren, Phys. Rev. B **31**, 6216 (1985); R. Baudoing, Y. Gauthier, M. Lundberg, and J. Rundgren, J. Phys. C **19**, 2825 (1986).
[21] P. Weigand, P. Novacek, G. van Husen, T. Neidhart, and P. Varga, Surf. Sci. **269/270**, 1129 (1992).
[22] W. Hofer, Fresenius J. Anal. Chem. (to be published).
[23] G. Tréglia and B. Legrand, Phys. Rev. B **35**, 4338 (1987).
[24] C. E. Dahmani, M. C. Cadeville, J. M. Sanchez, and J. L. Morán-López, Phys. Rev. Lett. **55**, 1208 (1985).
[25] Y. Gauthier and R. Baudoing, in *Surface Segregation Phenomena* (Ref. [19]), p. 169.

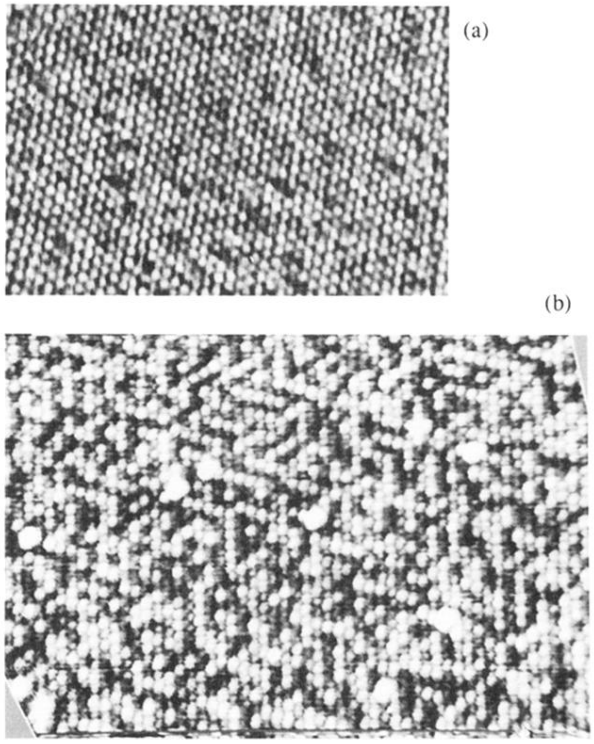

FIG. 1. STM constant current topographs of the (111) surface of a $Pt_{25}Ni_{75}$ single crystal. Tunneling voltage/current and sample treatment: (a) 0.5 mV/7 nA, thoroughly cleaned; (b) 5 mV/16 nA, less cleaning. Image sizes are 100 Å×70 Å and 125 Å×100 Å. Both images have been slightly high-pass filtered; image (b) has been distorted to correct for drift and creep of the STM.